Original Article

MOLECULAR METABOLISM

# A practical and robust method to evaluate metabolic fluxes in primary pancreatic islets

**Debora S. Rocha[1], Antonio C. Manucci[1], Alexandre Bruni-Cardoso[1], Alicia J. Kowaltowski[1], Eloisa A. Vilas-Boas[1,2,*]**

## ABSTRACT

**Objective:** Evaluation of mitochondrial oxygen consumption and ATP production is important to investigate pancreatic islet pathophysiology. Most studies use cell lines due to difficulties in measuring primary islet respiration, which requires specific equipment and consumables, is expensive and poorly reproducible. Our aim was to establish a practical method to assess primary islet metabolic fluxes using standard commercial consumables.

**Methods:** Pancreatic islets were isolated from mice/rats, dispersed with trypsin, and adhered to pre-coated standard Seahorse or Resipher microplates. Oxygen consumption was evaluated using a Seahorse Extracellular Flux Analyzer or a Resipher Real-time Cell Analyzer.

**Results:** We provide a detailed protocol with all steps to optimize islet isolation with high yield and functionality. Our method requires a few islets per replicate; both rat and mouse islets present robust basal respiration and proper response to mitochondrial modulators and glucose. The technique was validated by other functional assays, which show these cells present conserved calcium influx and insulin secretion in response to glucose. We also show that our dispersed islets maintain robust basal respiration levels, in addition to maintaining up to 89% viability after five days in dispersed cultures. Furthermore, OCRs can be measured in Seahorse analyzers and in other plate respirometry systems, using standard materials.

**Conclusions:** Overall, we established a practical and robust method to assess islet metabolic fluxes and oxidative phosphorylation, a valuable tool to uncover basic β-cell metabolic mechanisms as well as for translational investigations, such as pharmacological candidate discovery and islet transplantation protocols.



**Keywords** Mitochondrial respiration; Oxidative phosphorylation; Oxygen consumption; Pancreatic islets

## 1. PANCREATIC β-CELLS AND MITOCHONDRIAL RESPIRATION

Glucose-stimulated insulin secretion (GSIS) [1] begins with glucose entry into β-cells through specific transporters. It is then rapidly phosphorylated by glucokinase, generating glucose-6-phosphate, which proceeds through the glycolytic pathway, generating pyruvate. Inside mitochondria, pyruvate is converted into acetyl-CoA and completely oxidized by the tricarboxylic acid (TCA) cycle, which, together with oxidative phosphorylation, efficiently generates ATP. Increased ATP/ADP ratios lead to closure of ATP-sensitive potassium channels ($K_{ATP}$) at the plasma membrane, with subsequent membrane depolarization, opening of membrane voltage-sensitive calcium ($Ca^{2+}$) channels, $Ca^{2+}$ influx and activation of exocytotic machinery, culminating in insulin release.

Since pancreatic β-cells efficiently couple glucose metabolism to insulin release through mitochondrial electron transport and ATP production [2,3], studying oxygen consumption rates (OCR) in *ex vivo* islets is of great interest. Most studies use cell lines, while few existing studies with primary islets [4–10] use specific equipment and consumables that are expensive, complicated to use, and yield poorly reproducible results. While cell lines are an important tool, primary islets are a much more robust model to evaluate β-cell function.

Here, we briefly discuss methods available to measure isolated islet oxygen consumption and their limitations. We describe in detail a new and practical protocol to assess isolated pancreatic islets oxygen consumption rates using two different systems (Seahorse Extracellular Flux Analyzer and Resipher Real-time Cell Analyzer) and standard

[1]Departamento de Bioquímica, Instituto de Química, Universidade de São Paulo, SP, Brazil [2]Departamento de Análises Clínicas e Toxicológicas, Faculdade de Ciências Farmacêuticas, Universidade de São Paulo, São Paulo, SP, Brazil

*Corresponding author. Clinical and Toxicological Analysis Department, Pharmaceutical Sciences Faculty, University of Sao Paulo, Sao Paulo, SP, Brazil. E-mail: elovilasboas@usp.br (E.A. Vilas-Boas).

*Abbreviations:* $K_{ATP}$, ATP-sensitive potassium channels; Diaz, diazoxide; Glib, glibenclamide; Glu, glucose; GSIS, glucose-stimulated insulin secretion; HBSS, Hanks' Balanced Salt Solution; KH, Krebs Henseleit; OCR, oxygen consumption rates; TCA, tricarboxylic acid

Received January 15, 2024 • Revision received February 22, 2024 • Accepted March 17, 2024 • Available online 21 March 2024

https://doi.org/10.1016/j.molmet.2024.101922

 

microplates. The technique was optimized for both mice and rats, and results in increased islet yield and robust reproducibility.

## 2. EXISTING METHODS TO MEASURE ISLET OXYGEN CONSUMPTION

Respiration can be measured using Oroboros high-resolution oxygraphy, where islets are suspended and their OCRs followed over time. This is an indisputably robust method, however, there are two disadvantages in the case of islets. Measurements are made in 0.5 mL or 2 mL chambers, large volumes that require a high number of cells. Islet isolation is a multi-step protocol and the yield depends on several parameters, but, since islets are around 2% of all pancreatic cells, the yield is low. In our hands, basal OCRs were very low using up to 80 rat islets in a 2 mL chamber. Indeed, the required number of islets seems to be much higher, around 250 mouse islets per mL [4], which results in large use of animals, as one mouse yields approximately 200—350 islets, while one rat yields approximately 400—600 islets. In addition, the constant stirring, necessary during oxygen electrode measurements to ensure proper oxygen diffusion, can damage the islets, leading to cell dispersion and decreased viability [5]. Specific devices have been developed to overcome this, such as a 3D-printed chamber to stabilize the islets during Oroboros measurements [5]. As an alternative to Oroboros, other strategies have also been developed, such as an islet-on-a-chip microfluidic device that allows OCR measurements at the same time as $Ca^{2+}$ imaging of individual islets [6]. However, these devices are not readily available commercially.

The Seahorse Extracellular Flux system, widely available in most major research centers, was designed specifically for adherent cells, and has enhanced sensitivity while also avoiding stirring damage. However, the spheroid arrangement of islets is not adequate for use in its standard plate-based systems, in which the sensors are located close to the adherent plate surface during measurements, to enhance sensitivity.

There are specific, commercially available, Seahorse 96-well microplates for spheroids, with round bottoms which could favor placing islets in the center. However, working with 3D structures can be tricky, and several adjustments and precautions must be taken into account depending on the cell type used [11]: some researchers place the islets under a microscope to orient pipetting [7], centrifuge islets after pipetting [7,8], and in all cases pre-coating of the plates is required for the islets to properly adhere to the bottom and avoid movement during measurement [7—9]. Even with these precautions, islets may still detach during mixing and measuring steps. In addition, a special thermal tray compatible with the spheroid microplate is required for the measurements, so the equipment must be reserved for spheroid plates, and cannot interchangeably use other plates adequate for most adherent cell types.

Another possibility are 24-well Seahorse microplates specifically designed for islets [10]. Islets are placed in a depression at the bottom of the well, and each well has a polycarbonate grid to lock in the islets and keep them from detaching during mixing and measuring steps. Of note, the spheroid microplates can only be used in 96-well Seahorse systems, while islet capture microplates can only be used in 24-well Seahorse systems, limiting the choice of use for researchers who have access to only one of these analyzers. Previous attempts were also performed using matrigel in a poly-D-lysine-coated standard XF96 microplate [12]. However, this is a difficult protocol to follow that still has disadvantages similar to those mentioned above.

Currently, new strategies allow measurements of OCRs directly in standard well plates over days in culture. This technique and equipment, named Resipher, is suitable for adherent cells and has never been tested in islets before, to our knowledge.

Overall, several limitations that hinder robust and reproducible OCR assessment in primary islets persist today, and result in restricted measurements of this important functional parameter. These limitations are mostly due to the high number of islets required for the measurements, loss of viability during the measurements, special devices and consumables that are tricky to use and expensive, in addition to poor reproducibility between replicates. We present here a detailed protocol of a practical method that allows robust and reproducible OCR measurements using a relatively low number of islets and standard materials, which we hope will stimulate and facilitate future studies.

## 3. OPTIMIZATION OF RODENT ISLET ISOLATION

We isolated islets from 8 to 12 week-old C57BL/6NTac male mice and Sprague Dawley female rats. Animals were bred and housed in the animal facility of the Chemistry Institute of the University of São Paulo in collective cages (max 5/cage) at controlled temperatures (23 °C) in a 12-12 h light/dark cycle with free access to food/water. Procedures were in accordance with the Ethical Principles of Animal Manipulation (protocols CEUA-IQ/USP196/2021 and 244/2022).

### 3.1. Pancreatic islet isolation

Lacy et al., in 1967 [13] originally developed a protocol using a collagenase solution in Hanks' buffer, highlighting the importance of clamping the Ampulla of Vater, where bile and pancreatic ducts meet. This prevents collagenase leakage into the intestine, avoiding inadequate inflation of the pancreas [13]. This protocol has been optimized since then, leading to greater islet yields per animal. Corbin et al. [14] highlighted the importance of using adequate collagenase, with types V, XI, and P collagenases being the most suitable. Centrifugation, discarding the supernatant, and washing with a fresh buffer are additional crucial steps. Lacy et al. [13] compared the effects of centrifugation to simple gravity sedimentation, leading to an average yield gain from 100 to 300 islets/mouse, close to the number obtained by us. However, they also pointed out that sucrose gradient centrifugation may be harmful to the islet function.

Salvalagio et al. [15] compared Ficoll gradients and cell strainer filtrations in regard to the yield and functionality. The use of a Ficoll gradient was less effective in comparison to filtration when evaluating the number of islets, GSIS, and purity. Also, islets isolated by filtration restored normoglycemia one day after transplantation into diabetic mice, while islets isolated by Ficoll needed 6—7 days for the same result. Regardless of the method used, manual collection significantly increases the purity of the islets.

All steps involved in islet isolation are relatively simple, but require practice by the researchers, and prior practice implies better effectiveness and speed [16]. Thus, a pilot experiment is mandatory to ensure a reasonable average number of islets and to avoid discarding animals due to lack of practice. Importantly, the time between the death of the animal and the separation of the endocrine and exocrine tissues has great impact on maintaining the viability and functionality of the islets. When using more than one animal per day, kill one at a time and isolate the tissue as freshly as possible. Finally, the age of the animals also impacts on yield, with higher yield values in older animals compared to juveniles [14].

### 3.2. Pancreatic islet isolation — optimized protocol

1. Anesthetize the animals as recommended by the local ethical committee. We used 70 mg/kg ketamine, 10 mg/kg xylazine, and

 

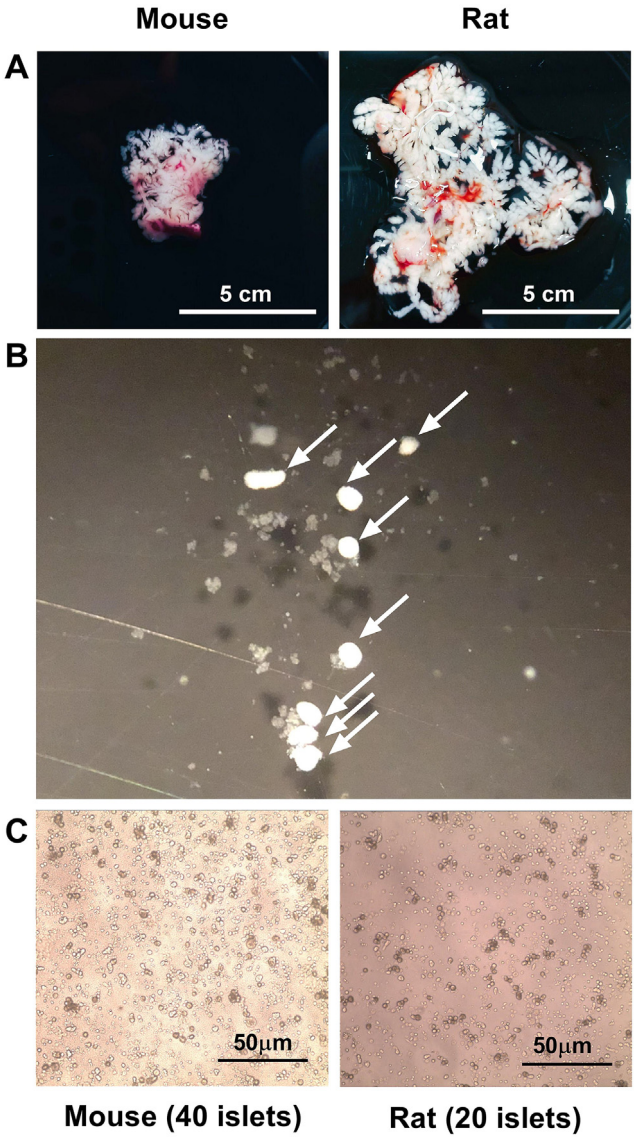


**Figure 1: Pancreas isolation, islet dispersion, and culture**. **(A)** After pancreas dissection and full inflation, whole mouse and rat pancreases can be visualized macroscopically. **(B)** After exocrine digestion with trypsin, isolated islets can be visualized using a stereomicroscope. **(C)** Dispersed and adhered islet cells in culture can be visualized using a microscope after hand-picking, dispersion with trypsin, and overnight adhesion on a pre-coated microplate. Representative figures are shown.

**Table 2** — Composition of Hanks' Balanced Salt Solution (HBSS).

| | g/L | mM |
|---|---|---|
| **PART 1** | | |
| NaCl | 8.18 | 140 |
| KCl | 0.37 | 5 |
| $MgSO_4$ | 0.048 | 0.4 |
| $Na_2HPO_4$ | 0.017 | 0.1 |
| $KH_2PO_4$ | 0.054 | 0.4 |
| **PART 2** | | |
| $CaCl_2$ | 0.0838 | 0.75 |
| $NaHCO_3$ | 0.336 | 4 |
| D-Glucose | 1.8 | 10 |
| BSA | 2 | 0.2 % |
| P/S | 10 mL | — |

**Table 3** — Composition of Krebs Henseleit.

| | Final 500 mL | Final 1 L | Final 2 L |
|---|---|---|---|
| **Solution I** | | | |
| NaCl (0.46 M) | 13.44 g | 26.88 g | 53.77 g |
| **Solution II** | | | |
| $NaHCO_3$ (0.096 M) | 4.03 g | 8.06 g | 16.12 g |
| KCl (0.02 M) | 0.74 g | 1.48 g | 2.96 g |
| $MgCl_2$. 6 $H_2O$ (4 mM) | 0.41 g | 0.82 g | 1.64 g |
| **Solution III** | | | |
| $CaCl_2$. 2 $H_2O$ (4 mM) | 0.29 g | 0.58 g | 1.16 g |

2 mg/kg acepromazine, followed by cervical dislocation (mice) or cardiac puncture (rats).

**Caution:** Islet yield increases in freshly isolated pancreases (we obtained at least 100–250/mouse and 200–350/rat). When using more than one animal/day, anesthetize one at a time. Islet collection and separation from the exocrine tissue must be performed readily. Use a maximum of two rats or three mice/day/investigator.

2. Keep animal in *dorsal decubitus*, clean the abdominal area with 70% ethanol, and access the abdominal cavity.

**Caution**: Islets tend to stick to furs, so use 70% ethanol to wet the animal and keep surgical material clean.

**Note:** As mice and their respective ducts are small, use a stereomicroscope during steps 3 and 4.

3. Place the animal's head close to the surgeon in *dorsal decubitus.* Access the abdominal cavity and locate the common bile duct. Clamp the end of the Ampulla of Vater using a Spencer Wells forceps.

**Note:** Using a surgical line is also feasible.

**Table 1** — Comparison of different plate respirometry systems.

| | Islet microplate | Spheroid microplate | Dispersed cell measurements |
|---|---|---|---|
| **Compatible system** | Seahorse XF24 | Seahorse XF96 | Seahorse XF24 and XF96; Resipher |
| **Microplate** | Specific islet microplate | Specific spheroid microplate | Standard microplate |
| **Specialized consumables** | Islet capture screen insert tool (suggested) | Specific thermal tray for spheroid (required) | No |
| **Islets per condition** | 50–80 (rat or mouse) | 1–20 (mouse or human) | 20 (rat)<br>40 (mouse) |
| **Precoating required** | No | Yes | Yes |
| **Whole islet/dispersed cells** | Whole islets | Whole islets | Dispersed cells |
| **Centrifugation required** | No | Yes | No |
| **Allows microscopy** | No | No | Yes |

 

4. Make a small cut in the duct, not transposing it, in order to insert a needle (30G) and infuse with 5 mL (mice) or 15 mL (rat) of cold collagenase type V in Hanks' Balanced Salt Solution (HBSS, Table 2) (0.7 mg/mL).
   **Caution**: The collagenase solution must be sterile (filtered with 0.2 μm filter) and at 4—8 °C. Avoid bubbles and do not inject air into the tissue.
5. After full inflation, remove the whole pancreas carefully, to prevent it from breaking or allowing intestinal content to pour into the tissue.
   **Note:** Figure 1A shows a whole mouse and rat pancreas after full inflation.
   **Caution**: Avoid taking more than 15 min per animal.
6. Mince the tissue into small fragments using sharp scissors.
   **Caution**: Maintain the tissue-collagenase mixture at 4—8 °C if using more than one animal at a time.
7. Incubate the pancreases for 25 min at 37 °C (water bath) with gentle shaking for digestion of the exocrine tissue.
8. After incubation, shake the pancreas manually (do not vortex) until the tissue is dissociated into a homogenous solution.
9. Place the solution on ice to stop digestion.
10. Complete to a final 20 mL with HBSS (4—8 °C) (Table 2).
11. Centrifuge at 1200 rpm (185 g) for 3 min at 4 °C.
12. Carefully discard the supernatant, keeping a small part of the liquid phase to avoid tissue loss, and re-suspend the pellet with 20 mL of ice-cold HBSS buffer.
13. Steps 11 and 12 should be done thrice.
14. Put the solution in a dark background Petri dish, and collect islets manually to another plate with cold HBSS using a micropipette under a stereomicroscope, keeping everything, other than the stereomicroscope plate, on ice.
    **Note:** Figure 1B shows isolated islets in HBSS after handpicking, with a few digested exocrine tissue pieces. Arrows mark isolated islets, which are round, white structures surrounded by digested exocrine tissue.
    **Note:** Staining islets with special dyes is also possible to facilitate visualization, but not necessary.
    **Note**: Ficoll, Percoll, and sucrose gradients can also be used for purification, but islet viability and functionality may be lower when compared to handpicking.

### 3.3. Pancreatic islet dispersion and culture

An important limitation of using intact islets is that large islets often display insufficient oxygen diffusion toward the islet core, leading to central necrosis due to hypoxia [17,18]. This situation may be heightened when keeping islets for days in culture. In this paper, we chose to use dispersed islets adhered to standard flat-bottom Seahorse XF24 microplates. The three-dimensional structure of the pancreatic islet and the interaction between different endocrine cell types is important for its function; paracrine interactions impact on responses [19,20]. Therefore, although most dispersion protocols are relatively fast and simple, validation may be necessary to guarantee adequate functionality if interactions between cells are expected to participate in the biological phenomena studied (item 3.4).

#### 3.3.1. Pancreatic islet dispersion and culture — protocol

1. After handpicking, collect 20 (rats) or 40 (mice) islets in conic microtubes containing 300 μL cold trypsin—EDTA solution (0.25%).
   **Note:** The dispersion protocol was carried out on the same day as the isolation.
   **Note:** There is a natural tendency to choose the best islets first, so to minimize variations between replicates, collect the first same-sized 10—20 islets to all tubes, and then collect the final same-sized islets.
   **Note:** Use 20 rat islets or 40 mouse islets per well. We recommend at least 4 technical replicates per animal.
   **Note:** 20 islets from the wild type rats used are equivalent to approximately 22,500 to 44,500 cells, while 40 islets from the wild type mice used are equivalent to approximately 34,500 to 54,000 cells.
   **Note:** When using different Seahorse analyzers, the number of islets or cells should be adjusted. We used 15 rat islets in a XF96 analyzer and obtained robust respiration. Using less than 15 increased variability to the point in which it compromised the results (data not shown).
2. Incubate islets in trypsin at 37 °C for 2 min with gentle shaking.
3. Place the tubes immediately on ice and inactivate trypsin with 600 μL complete RPMI medium with 10% fetal bovine serum (FBS).
4. Centrifuge at 1200 rpm (185 g) for 1 min to pellet cells.
5. Discard the supernatant carefully with a micropipette and resuspend dispersed islets in 150 μL RPMI.
   **Note:** If necessary, use a spotlight to visualize the pellet and avoid discarding the islets with the supernatant.
6. Homogenize the pellet by pipetting up and down until complete visible dispersion.
7. Transfer the whole volume to cell culture plates previously coated with poly-L-lysine (item 3.3).
8. Let cells adhere overnight at 37 °C in a humidified atmosphere of 5% $CO_2$/95% air.
   **Note:** Figure 1C shows dispersed cells from mouse (left) and rat (right) pancreases.

### 3.4. Poly-L-lysine coating

Proper cell adhesion to the wells is of extreme importance, to avoid loss of cell adhesion during mixing and measuring steps. Here, all cell culture microplates were coated with poly-L-lysine (#P8920, Sigma) prior to use. We found that letting the cells adhere overnight, rather than for a few hours, ensures proper adhesion and reduces variability between replicates.

1. Add 50 μL/well of prediluted poly-L-lysine (0.001%) solution to the Seahorse XF24 microplate and incubate for at least 1 h at 37 °C.
2. Rinse wells twice with 200 μL/well sterile milliQ water.
3. Discard the water and let the wells dry at room temperature inside a laminar flow cabinet.
4. After completely dry, seal the plates with parafilm and reserve at 2—8 °C for up to 10 days.

### 3.5. Validation of the protocol by functional assays

#### 3.5.1. Glucose-stimulated insulin secretion (GSIS) in dispersed and intact islets

Glucose is imported into β-cells and metabolized, increasing intracellular ATP levels, leading to plasma membrane $K_{ATP}$ channel closure and depolarization, promoting voltage-sensitive $Ca^{2+}$ channel opening and $Ca^{2+}$ influx, recruiting secretory vesicle trafficking to the cell membrane (Figure 2A). We then evaluated GSIS of dispersed and adhered islets, as follows:

 

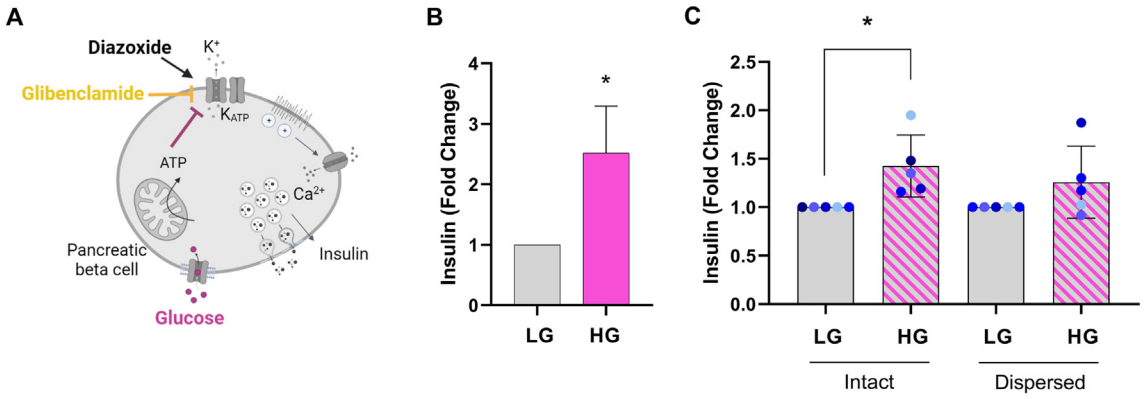


**Figure 2: Glucose-stimulated insulin secretion in dispersed and adhered mouse and rat islets. (A)** Physiological and pharmacological mechanisms involved in pancreatic β-cell insulin secretion. Glucose **(pink)** is taken up into the β-cell by a specific glucose transporter (GLUT2), independently of insulin. Glucose metabolism leads to increased intracellular ATP levels, and consequently plasma membrane ATP-sensitive potassium channel ($K_{ATP}$) closure and plasma membrane depolarization, voltage-sensitive $Ca^{2+}$ channel opening, $Ca^{2+}$ influx, insulin vesicle trafficking to the cell membrane, and insulin release. Glibenclamide **(yellow)** promotes $K_{ATP}$ closure and diazoxide **(black)**, $K_{ATP}$ opening, leading, respectively, to an increase and a decrease in insulin secretion. Created with BioRender.com. **(B)** Insulin secretion (Fold change) of dispersed and adhered mouse islets in response to glucose. Results are mean ± SEM of 5 mice. *p < 0.05 using paired Student's t test. **(C)** Insulin secretion (Fold change) in response to glucose of whole rat islets versus dispersed rat islets from the same animals. Results are mean ± SEM of 5 rats (each animal is represented by a different color). *p < 0.05 using paired Student's t test.

1. After cells properly adhere overnight, replace culture medium supernatant by 150 μL Krebs Henseleit (KH) buffer (Table 3) containing 2.8 mM (for mice) or 5.6 mM glucose (for rats).
2. Preincubate at 37 °C for 30 min.
3. Discard the supernatant and replace it with 150 μL kH buffer with low (5.6 mM) or high (20 mM) glucose concentrations.
4. Incubate at 37 °C for 60 min.
5. Collect the supernatant in fresh conic tubes and store at −20 °C.
6. Remove any remaining buffer and lyse cells with 30 μL of RIPA buffer.

   **Note**: The samples, insulin-containing supernatants, and plates with RIPA-lysed cells can be stored at −20 °C for up to one month.
7. Quantify total protein content using the BCA Pierce protocol.
8. Measure insulin by enzyme-linked immunosorbent assay (ELISA) (EZRMI-13K, Merck Millipore Corporation, Billerica, USA).

   **Note:** Several commercial kits are currently available to measure insulin. Before purchasing the kit, make sure that the standard curve range is appropriate for your samples.

   **Note:** Insulin can also be measured by radioimmunoassay, Fluorescence Resonance Energy Transfer (FRET), or High-Performance Liquid Chromatography (HPLC).

An increment from 5.6 mM to 20 mM glucose led to robust insulin secretion increases in mouse samples (Figure 2B), confirming that our protocol provides fully functional islets. We compared the response to glucose with an equivalent number of intact and dispersed rat islets from the same animal (Figue 2C). We show that both intact and dispersed rat islets have similar patterns of insulin secretion in terms of fold change, however dispersed islets had increased variability in high glucose. We thus suggest that, when using dispersed islets, the number of replicates should be increased to minimize the variability within the group.

### 3.5.2. Calcium ($Ca^{2+}$) influx in response to different modulators in dispersed islets

Next, we evaluated $Ca^{2+}$ signaling in response to different modulators (glucose, glibenclamide, and diazoxide). Glibenclamide is a $K_{ATP}$ -channel blocker, inducing membrane depolarization and voltage-sensitive $Ca^{2+}$ channel opening, resulting in $Ca^{2+}$ influx. On the other hand, diazoxide is a $K_{ATP}$ channel opener, decreasing $Ca^{2+}$ influx (Figure 2A).

After overnight incubation in 30 mm glass dishes previously coated with poly-L-Lysine, dispersed islet cells were incubated for 30 min at 37 °C with Fura-2 AM and then checked for $Ca^{2+}$ influx. Fura-2 AM fluorescence, which ratiometrically indicates cytosolic $Ca^{2+}$ levels, was detected using a Leica DMi8 wide-field fluorescence microscope operated with LASX Software (Leica Microsystems) at 37 °C and 5% $CO_2$/95% air. Cells were imaged under basal conditions in HBBS buffer with low glucose (5.6 mM) for 5 min, followed by addition of i) high glucose (final 20 mM); ii) 10 μM glibenclamide ($K_{ATP}$ channel blocker); iii) 250 μM diazoxide ($K_{ATP}$ channel opener) + high glucose (final 20 mM). A filter wheel installed in the light source permitted Fura2 fluorescence excitation at 340 nm ($Ca^{2+}$-bound) or 387 nm ($Ca^{2+}$-free), with emission at 510 nm. Mouse and rat islets were imaged for 15 and 20 min respectively. Images were analyzed using ImageJ FIJI Software. The steps of this protocol were performed as follows:

1. After cells properly adhere overnight, incubate cells for 30 min with 4 μM of Fura-2 AM at 37 °C in complete RPMI medium.
2. With a fluorescence microscope at 37 °C, in controlled atmosphere (5% $CO_2$/95% air), register basal fluorescence ratios for at least 5 min under low glucose (5.6 mM) conditions.
3. After 5 min (basal fluorescence), add the stimulus (physiological or pharmacological) and continue registering the fluorescence for 15—20 min.

   **Note:** The duration varies according to the stimulus used.

As seen in Figures 3—4, cells responded to glibenclamide by rapidly increasing cellular $Ca^{2+}$ influx, and to glucose in a more gradual manner. The gradual increase in response to glucose, in contrast to the instantaneous effect of glibenclamide, has different possible explanations. Glibenclamide has a direct effect on $K_{ATP}$ channels, while glucose needs to be intracellularly metabolized. Another possibility may be related to particularities among different β-cell populations, with responses faster than others; since the sample signal comes from

 

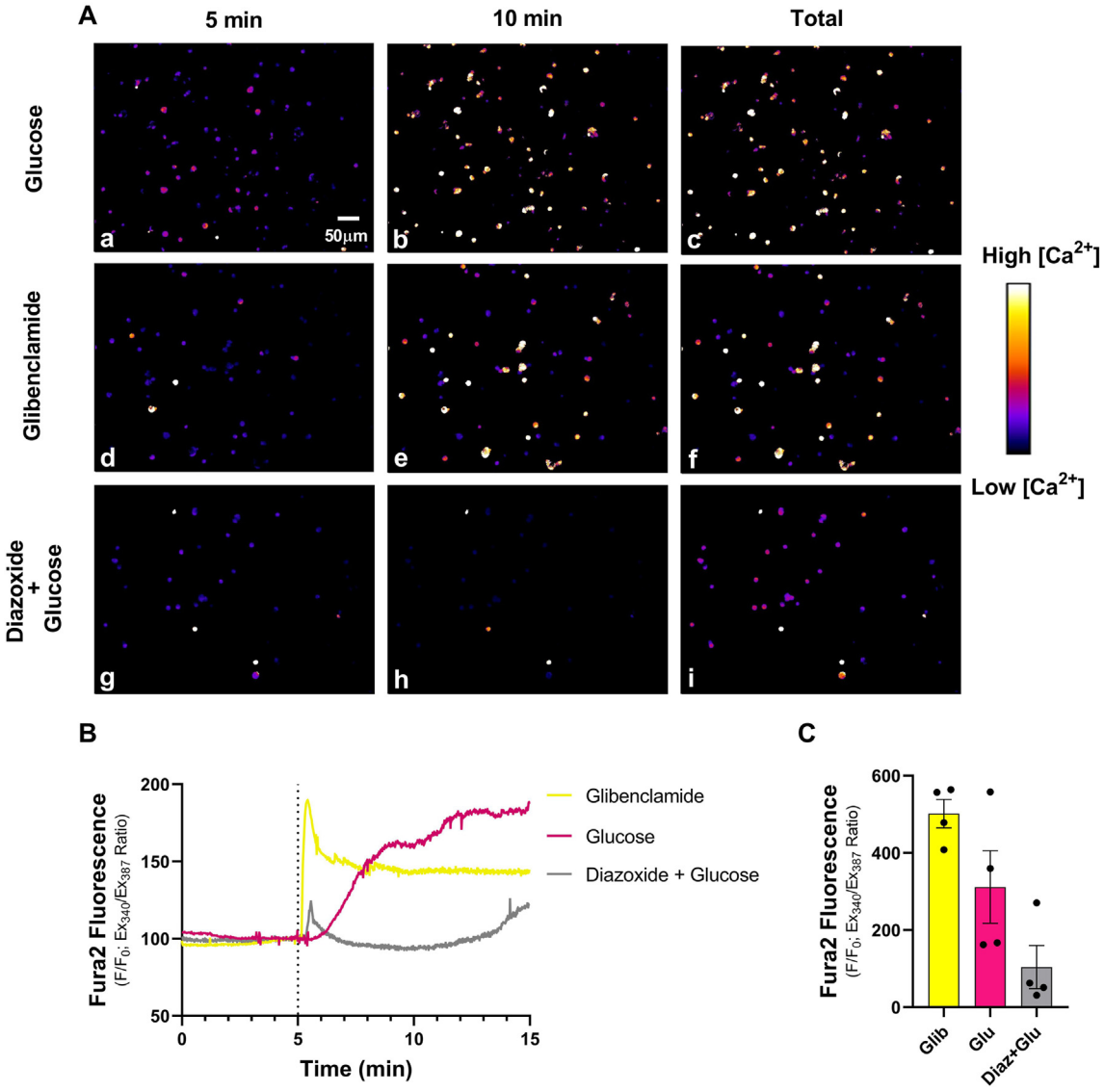


**Figure 3: Calcium influx assay in dispersed and adhered mouse islets**. **(A)** Live imaging of dispersed and adhered islet cells under basal conditions with low glucose (5.6 mM), followed by addition of high glucose (final 20 mM); 10 μM glibenclamide; or 250 μM diazoxide + high glucose (20 mM). Representative Fura2-AM fluorescence ratios (340/387 nm) at 5 min, 10 min and full trace with glibenclamide **(a,b,c)**; glucose **(d,e,f)** or diazoxide + high glucose **(g,h,i)**. Fluorescence was measured at baseline for 5 min, followed by additions indicated, up to 15 min total. **(B)** Representative $Ca^{2+}$ influx curves. **(C)** Fura2-AM fluorescence ratio (340/387 nm) quantifications. Glucose **(pink)**; glibenclamide **(yellow)** and diazoxide + glucose **(gray)**. Results are mean ± SEM of 4 animals.

the sum of these populations, the increment is gradual. It has been previously shown that individual dispersed cells have large variabilities in terms of $Ca^{2+}$ influx in response to glucose, but the sum of responses of all cells is similar to that of intact islets [21]. As our main aim was not to evaluate different responses among different cell types, we also considered the sum of responses from all dispersed cells, but would like to emphasize that the dispersed model renders itself amenable to studies involving heterogeneity, another advantage relative to bulk islet experiments. Finally, in the presence of diazoxide, glucose did not lead to $Ca^{2+}$ influx. Our results, therefore, show that cell dispersion and adhesion is an interesting tool for populational analysis of these cells, isolating the paracrine component from cell-to-cell communication. Furthermore, our results indicate that the expected physiological and pharmacological signaling pathways are preserved in the dispersed islet protocol, although, obviously, there is no guarantee that physiological responses are completely maintained among different cell types and beta cell subpopulations. Thus, we underlie that, while the dispersion protocol may not be suitable for and substitute all functional assays, we believe it is a practical method with ample and diverse applicability. Next, we evaluated if the protocol was adequate for metabolic flux analysis.

### 3.6. Oxygen consumption in dispersed islets

#### 3.6.1. Seahorse Extracellular Flux Analyzer (XF24 and XF96)

After overnight incubation on Agilent Seahorse XF24 or XF96 cell culture microplates previously coated with poly-L-lysine, OCRs were measured using a Seahorse Extracellular Flux Analyzer (Agilent Technologies, Santa Clara, CA, USA).

 

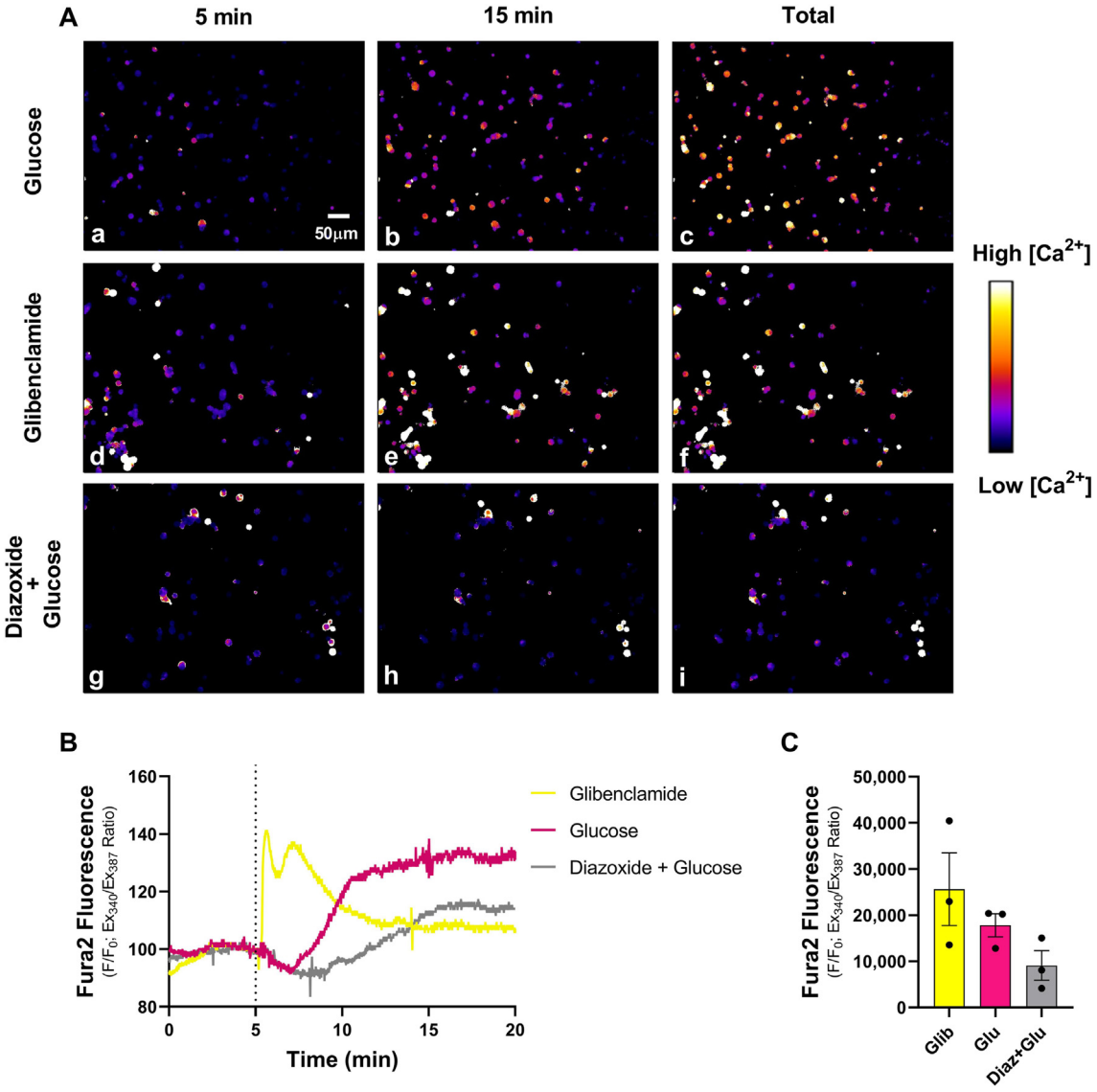


**Figure 4: Calcium influx assay in dispersed and adhered rat islets**. **(A)** Live imaging of dispersed and adhered islet cells under basal conditions with low glucose (5.6 mM), followed by addition of high glucose (final 20 mM); 10 µM glibenclamide; or 250 µM diazoxide + high glucose (20 mM). Representative Fura2-AM fluorescence ratios (340/387 nm) at 5 min, 15 min and full traces with glibenclamide **(a,b,c)**; glucose **(d,e,f)** or diazoxide + high glucose **(g,h,i)**. Fluorescence was measured at baseline for 5 min, followed by additions indicated, up to 20 min total. **(B)** Representative $Ca^{2+}$ influx curves. **(C)** Fura2-AM fluorescence ratio (340/387 nm) quantifications. Glucose **(pink)**; glibenclamide **(yellow)** and diazoxide + glucose **(gray)**. Results are mean ± SEM of 3 animals.

**Note:** Include cell-free wells with the same medium for background correction.

1. One day prior to the assay: hydrate Seahorse cartridge with appropriate calibrant solution overnight at 37 °C in a humidified incubator without $CO_2$.
2. Replace RPMI complete medium by 500 µL (XF24) or 180 µL (XF96) RPMI containing 1% penicillin/streptomycin (P/S) and 5 mM HEPES (without FBS nor bicarbonate).

   **Note:** Commercially available Seahorse media are also available.
3. Incubate cells for 1 h at 37 °C in a humidified incubator without $CO_2$.
4. Prepare working solutions and pipette solutions at ports.
5. Set the equipment: select different groups and different injections according to the protocol.

   **Note:** Select cell-free wells for background correction.

**Note:** To avoid cell detachment, we adjusted the timepoints to 1 min mixing + 2 min waiting + 3 min of measurements.

**Note:** We tested two protocols:

i) Basal respiration in 10 mM glucose followed by the standard Mito stress test [22].

ii) Basal respiration in 5.6 mM glucose, addition of high glucose in port A (final concentration: 20 mM), followed by the Mito stress test.

**Note:** Mito stress test injections for XF24: a) oligomycin (final 2 µM); b) CCCP (final 6 µM); c) rotenone and antimycin (R/AA, final 1 µM each).

**Note:** Mito stress test injections for XF96: a) oligomycin (final 1 µM); b) CCCP (final 2 µM); c) rotenone and antimycin (R/AA, final 1 µM each).

 

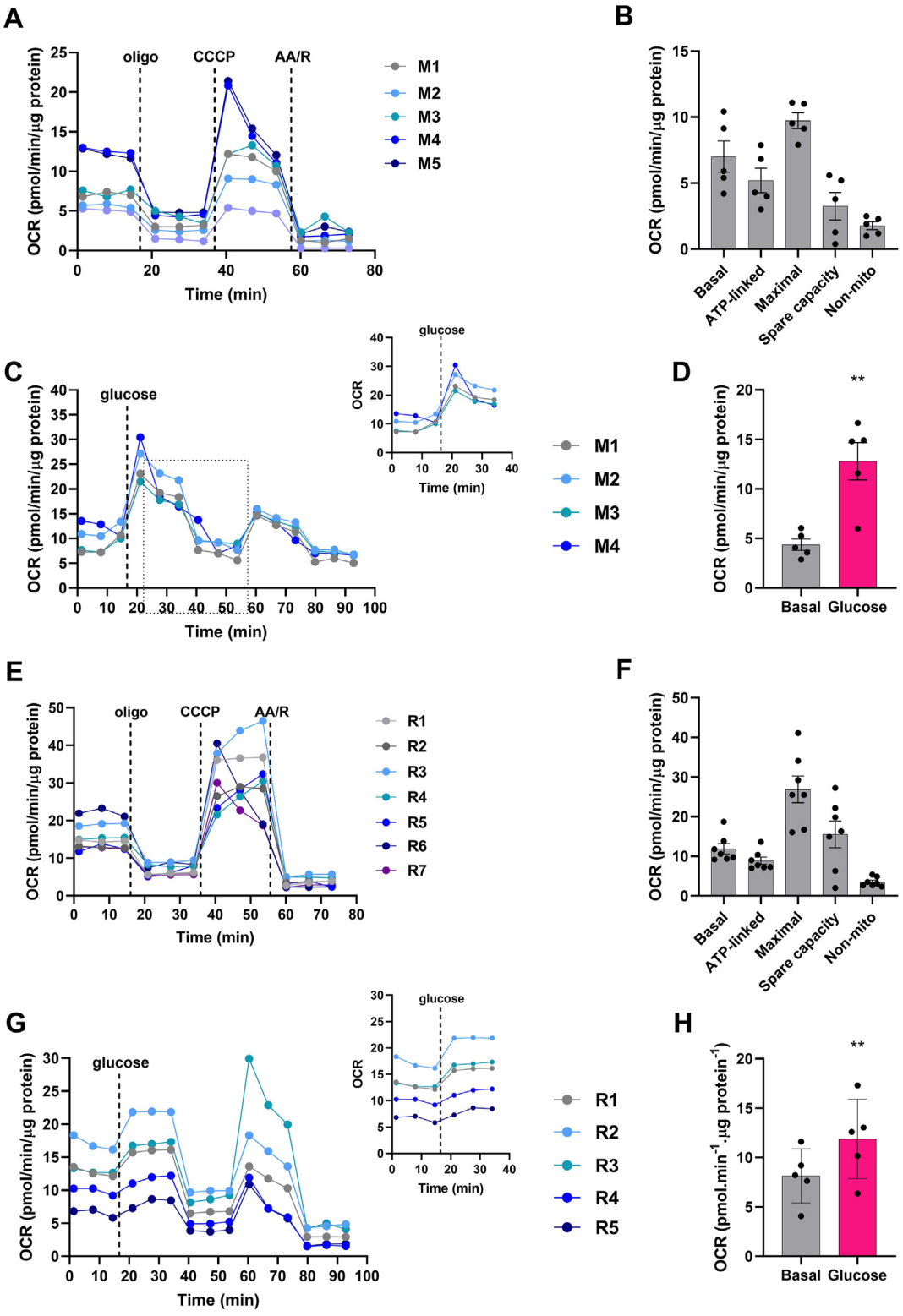


**Figure 5: Oxygen Consumption Rates (OCRs) in dispersed and adhered mouse and rat islets using an XF24 Seahorse Extracellular Flux Analyzer**. **(A)** OCR curves of 40 dispersed mouse islets in response to mitochondrial modulators oligomycin (2 µM), CCCP (6 µM) and Antimycin + Rotenone (1 µM each). **(B)** Quantification of mean basal, ATP-linked, maximal, and non-mitochondrial respiration. **(C)** OCR curves in response to glucose and mitochondrial modulators. Insets represent the magnified area indicated by the dotted lines. **(D)** Quantification of the mean OCR value. Results are mean ± SEM of 5 **(A—B)** or 4 **(C—D)** mice. M1-M5 represent the values of individual animals used. $^{**}p < 0.01$ using paired Student's t test. **(E)** OCR curves of 20 dispersed rat islets in response to mitochondrial modulators oligomycin (2 µM), CCCP (6 µM) and Antimycin + Rotenone (1 µM each). **(F)** Quantification of mean basal, ATP-linked, maximal, non-mitochondrial respiration, and spare capacity. **(G)** OCR curves in response to glucose and mitochondrial modulators. Insets represent the magnified area indicated by the dotted lines. **(H)** Quantification of the mean OCR value. Results are mean ± SEM of 7 **(E—F)** or 5 **(G—H)** rats. R1-R7 represent the values of individual animals used. $^{**}p < 0.01$ using paired Student's t test.

 

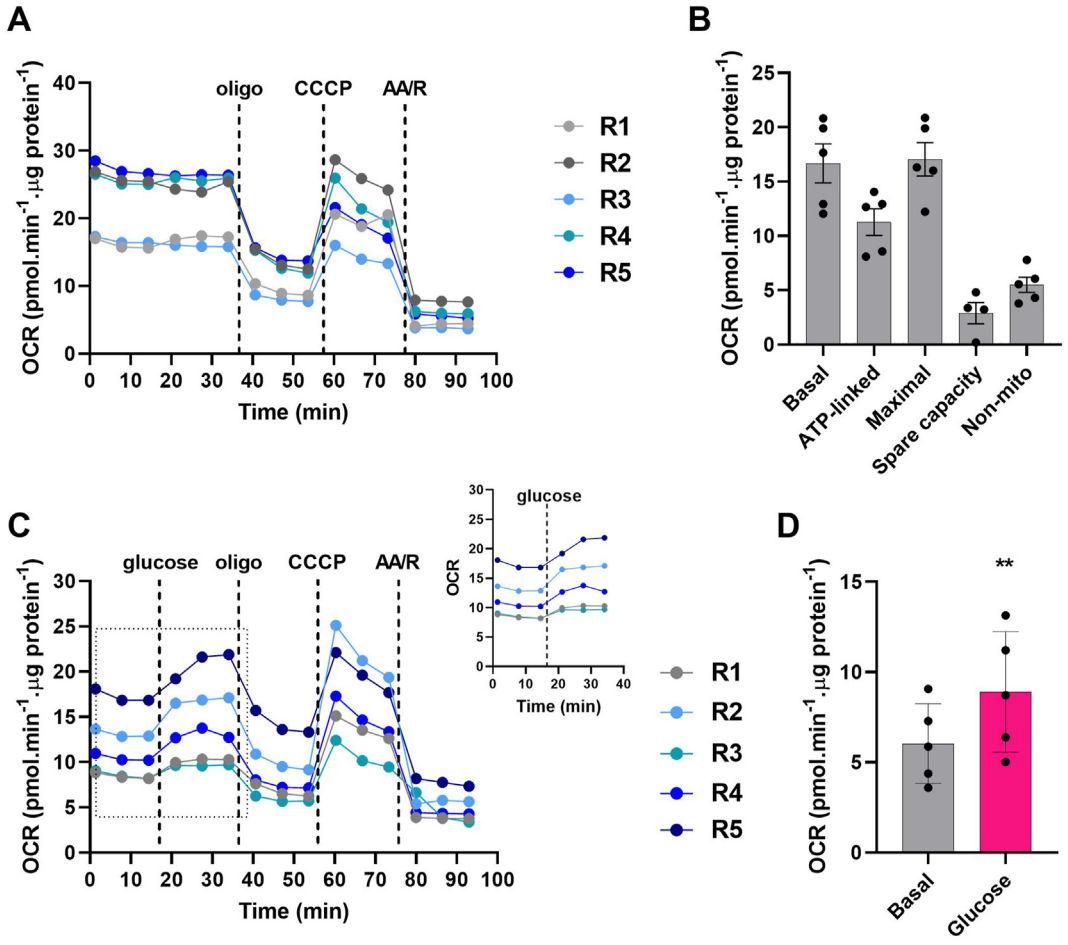


**Figure 6: Oxygen Consumption Rates (OCRs) in dispersed and adhered rat islets using an XF96 Seahorse Extracellular Flux Analyzer.** **(A)** OCR curves of 15 dispersed rat islets in response to mitochondrial modulators oligomycin (1 µM), CCCP (2 µM), and Antimycin + Rotenone (1 µM each). **(B)** Quantification of mean basal, ATP-linked, maximal, and non-mitochondrial respiration and spare capacity. **(C)** OCR curves in response to glucose and mitochondrial modulators. Insets represent the magnified area indicated by the dotted lines. **(D)** Quantification of the mean OCR value. Results are mean ± SEM of 5 rats. R1-R5 represent the values of individual animals used. $^{**}p < 0.01$ using paired Student's t test.

6. Place the cartridge in the Seahorse equipment for appropriate system calibration.
7. After 1 h incubation of cells and once calibration is ready, remove the microplate with the calibrant and place the microplate with cells in the equipment.
8. At the end of each experiment, remove the medium carefully and lyse cells with 30 µL (XF24) or 10 µL (XF96) RIPA buffer/well.
9. Quantify total protein using the BCA Pierce. Normalize OCRs obtained per amount of total protein in each well.

**Note:** Within each experiment, selecting same-sized islets decreases variability between replicates. However, there are variations between animals, because different animals have islets of different sizes.

**Note:** We used the XF24 and XF96 analyzers, as these are the available equipment in our facility, but our method, in principle, could be adapted for all Seahorse analyzers, including 8-well apparatuses.

Using a XF24 Seahorse analyzer, we find that both sample origins (mouse and rat) present the expected response to mitochondrial modulators (oligomycin, CCCP and antimycin + rotenone) (Figure 5A–B, E–F), as we observe a decrease in OCR after oligomycin addition (which inhibits ATP synthase), an increase after CCCP (which reduces the mitochondrial inner membrane potential, maximizing electron transport) and an expressive decrease after the injection of antimycin/rotenone (which inhibit electron transport). In response to glucose, we observe an expected and significant increase in OCR, which is more evident in mouse (Figure 5C–D) than rats (Figure 5G–H). We suggest that this difference may be due to the number of islets used (20 for rats and 40 for mice). However, and most importantly, the response is still clearly observed in both cases.

Interestingly, the prior addition of glucose decreases maximum OCRs in both mouse (Figure 5C–D) and rat samples (Figure 5G–H). This is expected, since these cells respond to glucose by promoting overt increases in $Ca^{2+}$ influx, which at high levels in mitochondria matrix may limit electron transport [23,24]. As a result, there is a decrease in the response to the uncoupler CCCP. This indicates that experimental designs should be developed specifically for different desired readouts: experiments in which maximized OCRs induced by uncouplers are important parameters should be conducted without a high glucose stimulus prior to the addition of CCCP.

We also obtained robust respiration and proper response to mitochondrial modulators and glucose using a XF96 Seahorse analyzer (Figure 6). Our results, therefore, show that our method is suitable for using both XF24 and XF96 Seahorse analyzers.

 

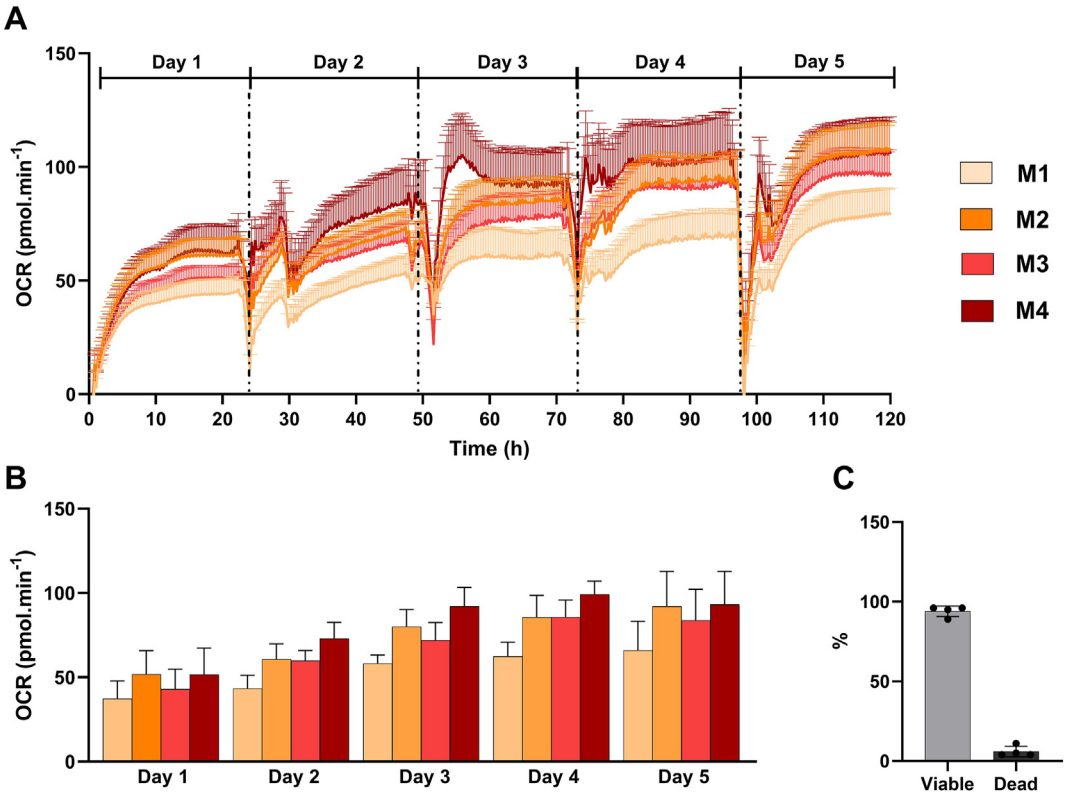


**Figure 7: Long term basal Oxygen Consumption Rates (OCRs) and cell viability in dispersed and adhered mouse islets using a Resipher analyzer. (A, B)** Basal OCRs of 40 dispersed mouse islets over five days in culture using a Resipher Real-time Cell Analyzer. Results are mean ± SEM of 4–5 technical replicates of 4 mice (M1, M2, M3 and M4). Dashed lines indicate medium change. **(C)** After OCR assessment over five days, viability was assessed and is presented in percentage (%) of viable and dead cells. Results are mean ± SEM of 4 mice.

### 3.6.2. Long term OCR measurement and cell viability

Next, we tested whether our dispersed method would be suitable for measuring OCRs in another plate respirometry system, the Resipher Real-time Cell Analyzer (Lucid Scientific, Atlanta, GA, USA), which allows basal OCR measurements in plated cells over days in culture.

After overnight incubation on standard 96-well culture microplates previously coated with poly-L-lysine, basal OCRs of dispersed islets of four mice were measured in complete RPMI medium (10 mM glucose, FBS, bicarbonate and HEPES) over five consecutive days in culture (Figure 7A,B). Five (mice 1, 2 and 3) or four (mouse 4) technical replicates were conducted.

**Note:** Include cell-free wells with the same medium for background correction.
**Note:** Change media every day.

Robust oxygen consumption was observed during all five days of data acquisition, with good sensitivity and low dispersion between samples (Figure 7A,B). A sample originating from each mouse was tripsinized and checked for cell viability with a Trypan-blue staining, using an automated cell counter (Countess™ 3 Automated Cell Counter, Thermo Fisher Scientific, Waltham, MA). We see that after six days of isolation, dispersion, and culture, to 89–96 % cells were viable (Fig. 7C).

In conclusion, our results show that, with our method, dispersed islets maintain robust basal respiration levels, in addition to maintaining high viability and metabolic activity after six days of isolation, dispersion, and culture. Furthermore, OCRs can be measured in Seahorse analyzers and in other plate respirometry systems using standard materials.

## 4. DIS(ADVANTAGES) OF DIFFERENT METHODS USING THE SEAHORSE EXTRACELLULAR FLUX SYSTEM

Mitochondrial OCRs can be measured with high resolution using two commercial setups: Oroboros Respirometers and Seahorse Extracellular Flux Analyzers. Although Oroboros Oxygraphy is a robust method, it requires a high number of islets per condition, meaning more than one animal per condition. Without the specific chamber to contain islets, it also compromises islet viability due to mechanical damage. Therefore, we consider the Seahorse Extracellular Flux System a more suitable method for islets. In Table 1, we compare the different Seahorse methods available with ours.

The specific islet microplate keeps the islets trapped underneath a grid, preventing them from floating away during the measurements (albeit not completely). On the other hand, it is more expensive than the standard microplate and is only compatible with the XF24 system. In addition, it requires some practice to position the grid on top of the wells, and is laborious and time consuming, with considerable variations between experiments. The spheroid microplate keeps the islets adhered when a proper precoating is used, although it does not guarantee that islets do not detach during measurements, leading to variations between replicates. It is more expensive than the standard microplate, is compatible only with the

 

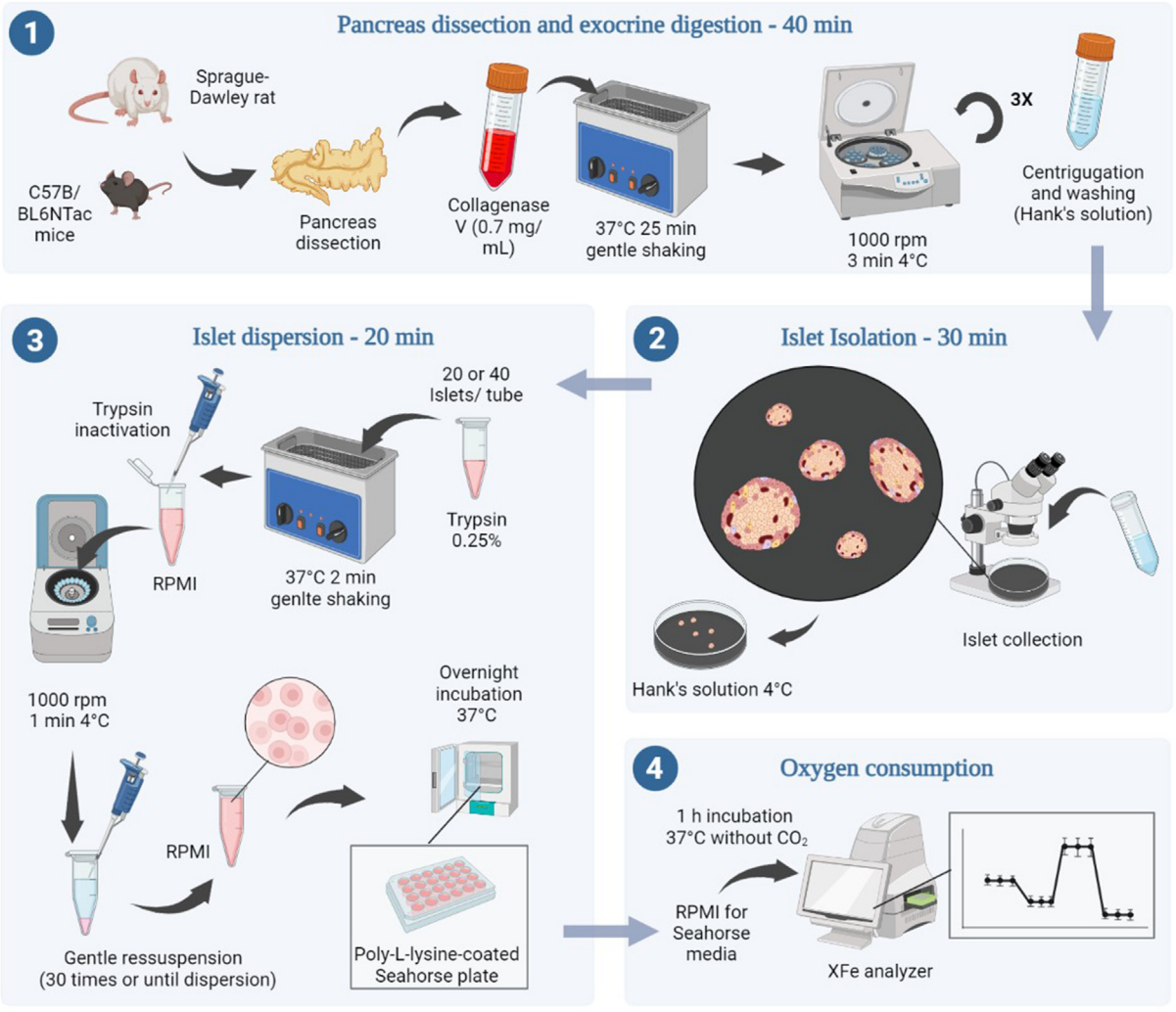


**Figure 8: A practical and robust method to evaluate *ex vivo* dispersed islet respiration**. Schematic workflow of all steps necessary to isolate, disperse, and culture mouse and rat islets, followed by oxygen consumption rate assays. Created with BioRender.com.

XF96 system, and needs a specific thermal tray. We propose a new and practical method using dispersed islets and the standard microplate (Figure 8), which is compatible with both XF24 and XF96 systems and does not need additional consumables or setups. Our method was developed for rodent islets, but in principle can also be used for human islets. In addition, this method also allows microscopy assays. This way, particularities between different endocrine cell types can be better explored, since the resolution of the microscope makes it possible to assess differences at the single cell level.

## 5. CONCLUSIONS

We optimized rodent islet isolation and functional analysis protocols using standard extracellular flux analysis equipment and consumables. Our method allows for increased islet yield and robust islet respiration measurements. In conclusion, the new protocol here described allows quantitative measurements of metabolic fluxes and oxidative phosphorylation, which are the cornerstone of new discoveries in beta cells. In this sense, it contributes toward the establishment of new cellular protocols, such as for cell transplantation, as well as the development of new pharmacological agents targeted to these cells.

## 6. BUFFERS AND CULTURE MEDIA COMPOSITION

### 6.1. Hanks' Balanced Salt Solution (HBSS) — for islet isolation

1. Add 800 mL of milliQ water to a suitable container;
2. Add NaCl, KCl, $MgSO_4$, $Na_2HPO_4$ and $KH_2PO_4$, according to Table 2;
3. Adjust pH to 6.3;
4. Add $CaCl_2$, $NaHCO_3$, D-glucose, bovine serum albumin, penicillin and streptomycin (P/S);
5. Adjust pH to 7.4 and final volume to 1 L;

 

6. Filter the solution using a 0.2 μm filter into a sterile flask;
7. Store at 4 °C until use.

### 6.2. Krebs Henseleit (KH) buffer — for islet isolation

1. Mix equal volumes of each solution (I, II + III) with same volume of milliQ water;
2. Adjust pH to 7.4, bubbling carbogen.
   OBS.: do not use acid or base to adjust pH.
3. Add 0.2 % BSA (2 g for a final 1 L).

### 6.3. RPMI 1640 culture medium

1. Supplement with bicarbonate (2 g/L), 10% FBS (100 mL for a final 1 L) and 1% P/S.
2. Adjust pH to 7.4 and filter using a 0.2 μm filter.
   **Note:** For cell cultures, we used media with 11.1 mM glucose and phenol red (#31800-022). For cell imaging, we used a media with 5.6 mM glucose and without phenol red (#103576-100).

### 6.4. Hanks' Balanced Salt Solution (HBSS) — for $Ca^{2+}$ imaging (#14175-095, Sigma)

1. Supplement with 2 mM $CaCl_2$ and 0.4 mM $MgSO_4$. To a final 30 mL HBSS, add 60 μL $CaCl_2$ 1 M and 12 μL $MgSO_4$ 1 M.
2. Adjust pH to 7.4.

## 7. TROUBLESHOOTING

See Table 4.

**Table 4 — Troubleshooting.**

| Problem | Possible reasons | Suggestions |
|---|---|---|
| Low islet yield | Inadequate shaking during exocrine digestion | Make sure you get the solution as homogeneous as possible, so that collagenase is in contact with the full tissue area. However, if you shake the solution too much or too hard, it can disrupt the islets and also decrease yield. |
| | Animals are too young | Prefer using adult animals (up to 4 months old), which have more and bigger islets than young individuals |
| | Islets with low viability | Anesthetize and dissect one animal at a time and avoid spending more than 15 min for dissection |
| | Inappropriate collagenase used for digestion | Use collagenase V (#C9263, Sigma) or P (#COLLP-RO), which are efficient for pancreas islet isolation |
| | Many protocol pauses before islets are separated from exocrine tissue | Make sure you have all materials and solutions on hand. Avoid delays, especially when islets are still mixed with exocrine tissue |
| Islet yield decreases between animals | Excessive number of animals on the same day experiment (more than 3) | Reduce the number of animals dissected in order to avoid expending more than 40 min in step 1; or increase the number of trained staff for islet collection |
| | Excessive time spent in step 2 (more than 30 min) | Make sure you get all materials and solutions ready before starting. Avoid delays, especially when islets are still mixed with exocrine tissue. |
| Poorly adhered cells | Incomplete dispersion | Make sure that the final resuspension of step 3 leads to a completely dispersed sample |
| | Plates not properly coated | Stock the coated plates for no more than 10 days until use. |
| | Islets in suspension | Replace the growth media for Seahorse media carefully to avoid dispersion. |
| | Plates not properly coated | Incubate the plates with poly-lysine solution for at least 1 h |
| Low OCR values | Too few islets per well | Use 40 islets per well for C57B/BL6NTac mice or 20 islets per well for Sprague—Dawley rats.<br>Be aware of species peculiarities and adapt the number to achieve consistent results |
| | Too much time spent in steps 1, 2 or 3, and too much time in contact with exocrine tissue, leading to a decreased islet viability | Use no more than 40 min for step 1, 30 min for step 2 and 20 min for step 3 for each animal |
| | Islets in suspension and, consequently, poor OCR and ECAR measurements | Replace the growth media for Seahorse media carefully to avoid dispersion. Decrease shaking and/or waiting time in Seahorse protocols |
| Large variation among replicates | Too few islets per well | Use 40 islets per well for C57B/BL6NTac mice or 20 islets per well for Sprague—Dawley rats.<br>Be aware of species peculiarities and adapt the number to achieve consistent results |
| | Too few experimental replicates for Seahorse analysis | Use at least 4 experimental replicates for each condition, considering the variance in the number of cells per dispersed islets |
| Decrease or absence of response to oxidative phosphorylation inhibition drugs | Inadequate concentration of oxidative phosphorylation inhibition drugs | Always titrate the drugs used in a pilot study |

 

## FUNDING

This work was supported mainly by the Fundação de Amparo à Pesquisa do Estado de São Paulo (FAPESP) under grant numbers 13/07937-8, 20/06970-5, 21/02481-2 and 21/04781-3 as well as the Conselho Nacional de Desenvolvimento Científico e Tecnológico (CNPq) and Coordenação de Aperfeiçoamento de Pessoal de Nível Superior (CAPES) line 001.

## AUTHORS' RELATIONSHIPS AND ACTIVITIES

The authors declare that there are no relationships or activities that might bias, or be perceived to bias, their work.

## CREDIT AUTHORSHIP CONTRIBUTION STATEMENT

**Debora S. Rocha:** Writing — review & editing, Writing — original draft, Investigation, Formal analysis, Conceptualization. **Antonio C. Manucci:** Investigation, Formal analysis. **Alexandre Bruni-Cardoso:** Formal analysis. **Alicia J. Kowaltowski:** Writing — review & editing, Writing — original draft, Supervision, Funding acquisition, Conceptualization. **Eloisa A. Vilas-Boas:** Writing — review & editing, Writing — original draft, Methodology, Investigation, Formal analysis, Conceptualization.

## ACKNOWLEDGMENTS

The authors thank Camille C. Caldeira da Silva for excellent technical assistance. We also acknowledge Silvânia M. P. Neves and her animal facility crew for exceptional expert animal care. We also acknowledge Dr Kin Lo from Lucid Scientific for the support with Resipher setup. We also acknowledge José Arimatéa de Oliveira Nery Neto and Meire Hiyane from Prof. Niels Olsen Saraiva Câmara for the assistance with the XF96 analyzer.

## DECLARATION OF COMPETING INTEREST

The authors declare that they have no known competing financial interests or personal relationships that could have appeared to influence the work reported in this paper.

## DATA AVAILABILITY

Data will be made available on request.

## REFERENCES

[1] Rorsman P, Ashcroft FM. Pancreatic β-cell electrical activity and insulin secretion: of mice and men. Physiol Rev 2018;98(1):117—214.
[2] Wiederkehr A, Wollheim CB. Mitochondrial signals drive insulin secretion in the pancreatic β-cell. Mol Cell Endocrinol 2012;353(1—2):128—37.
[3] Maechler P. Mitochondrial function and insulin secretion. Mol Cell Endocrinol 2013;379(1—2):12—8.
[4] Yamauchi Y, Nakamura A, Yokota T, Takahashi K, Kawata S, Tsuchida K, et al. Luseogliflozin preserves the pancreatic beta-cell mass and function in db/db mice by improving mitochondrial function. Sci Rep 2022;12(1):9740.
[5] Crowder JJ, Zeng Z, Novak AN, Alves NJ, Linnemann AK. Stabilization protects islet integrity during respirometry in the Oroboros Oxygraph-2K analyzer. Islets 2022;14(1):128—38.
[6] Regeenes R, Wang Y, Piro A, Au A, Yip CM, Wheeler MB, et al. Islet-on-a-chip device reveals first phase glucose-stimulated respiration is substrate limited by glycolysis independent on $Ca^{2+}$ activity. Biosens Bioelectron X 2023;13:100285.
[7] Taddeo EP, Stiles L, Sereda S, Ritou E, Wolf DM, Abdullah M, et al. Individual islet respirometry reveals functional diversity within the islet population of mice and human donors. Mol Metab 2018;16:150—9.
[8] Fukunaka A, Shimura M, Ichinose T, Pereye OB, Nakagawa Y, Tamura Y, et al. Zinc and iron dynamics in human islet amyloid polypeptide-induced diabetes mouse model. Sci Rep 2023;13(1):3484.
[9] Kim YK, Walters JA, Moss ND, Wells KL, Sheridan R, Miranda JG, et al. Zinc transporter 8 haploinsufficiency protects against beta cell dysfunction in type 1 diabetes by increasing mitochondrial respiration. Mol Metab 2022;66:101632.
[10] Wikstrom JD, Sereda SB, Stiles L, Elorza A, Allister EM, Neilson A, et al. A novel high-throughput assay for islet respiration reveals uncoupling of rodent and human islets. PLoS One 2012;7(5):e33023.
[11] Coltman NJ, Rochford G, Hodges NJ, Ali-Boucetta H, Barlow JP. Exploring mitochondrial energy metabolism of single 3D microtissue spheroids using extracellular flux analysis. J Vis Exp 2022;180.
[12] Taddeo EP, Alsabeeh N, Baghdasarian S, Wikstrom JD, Ritou E, Sereda S, et al. Mitochondrial proton leak regulated by cyclophilin D elevates insulin secretion in islets at nonstimulatory glucose levels. Diabetes 2020;69(2):131—45.
[13] Lacy PE, Kostianovsky M. Method for the isolation of intact islets of Langerhans from the rat pancreas. Diabetes 1967;16(1):35—9.
[14] Corbin KL, West HL, Brodsky S, Whitticar NB, Koch WJ, Nunemaker CS. A practical guide to rodent islet isolation and assessment revisited. Biol Proced Online 2021;23(1):7.
[15] Salvalaggio PR, Deng S, Ariyan CE, Millet I, Zawalich WS, Basadonna GP, et al. Islet filtration: a simple and rapid new purification procedure that avoids ficoll and improves islet mass and function. Transplantation 2002;74(6):877—9.
[16] Li DS, Yuan YH, Tu HJ, Liang QL, Dai LJ. A protocol for islet isolation from mouse pancreas. Nat Protoc 2009;4(11):1649—52.
[17] Komatsu H, Cook C, Wang CH, Medrano L, Lin H, Kandeel F, et al. Oxygen environment and islet size are the primary limiting factors of isolated pancreatic islet survival. PLoS One 2017;12(8):e0183780.
[18] Komatsu H, Kandeel F, Mullen Y. Impact of oxygen on pancreatic islet survival. Pancreas 2018;47(5):533—43.
[19] Hartig SM, Cox AR. Paracrine signaling in islet function and survival. J Mol Med 2020;98(4):451—67.
[20] Félix-Martínez GJ, Godínez-Fernández JR. A primer on modelling pancreatic islets: from models of coupled β-cells to multicellular islet models. Islets 2023;15(1):2231609.
[21] Scarl RT, Corbin KL, Vann NW, Smith HM, Satin LS, Sherman A, et al. Intact pancreatic islets and dispersed beta-cells both generate intracellular calcium oscillations but differ in their responsiveness to glucose. Cell Calcium 2019;83:102081.
[22] Gu X, Ma Y, Liu Y, Wan Q. Measurement of mitochondrial respiration in adherent cells by Seahorse XF96 Cell Mito Stress Test. STAR Protoc 2021;2(1):100245.
[23] Halestrap AP. Calcium, mitochondria and reperfusion injury: a pore way to die. Biochem Soc Trans 2006;34(Pt 2):232—7.
[24] Vilas-Boas EA, Cabral-Costa JV, Ramos VM, Caldeira da Silva CC, Kowaltowski AJ. Goldilocks calcium concentrations and the regulation of oxidative phosphorylation: too much, too little, or just right. J Biol Chem 2023;299(3):102904.

 